SUPPORTING INFORMATION

PREFERENTIAL ADSORPTION AND ACTIVITY OF MONOCOMPONENT CELLULASES ON LIGNOCELLULOSE THIN FILMS WITH VARYING LIGNIN CONTENT

Raquel Martín-Sampedro[&,†,], Jenni L. Rahikainen[#], Leena-Sisko Johansson[&], Kaisa Marjamaa[#], Janne Laine,[&] Kristiina Kruus[#], Orlando J. Rojas[&,$,*]*

[&] Department of Forest Products Technology, School of Chemical Technology, Aalto University, FI-00076 Aalto, Espoo, Finland.

[#] VTT Technical Research Centre of Finland, P.O. Box 1000, FI-02044 VTT, Espoo, Finland.

[$] Departments of Forest and Biomaterials and Chemical and Biomolecular Engineering, North Carolina State University, Raleigh, NC 27695, United States.

**Corresponding authors.*

[†]Present Address: Cellulose and Paper Laboratories. Forestry Products Department.

INIA-CIFOR, Ctra de La Coruña Km 7.5, 28040 Madrid, Spain

This document provides data supplementary to the main contribution. It contains information about purity of the enzymes used (Figure S1); AFM images and XPS data of bi-component films before and after deacetylation (Figure S2 and Table S1); results from empirical models related to binding and hydrolysis rate constants (Tables S2 and S3); QCM profiles for the shift of the (negative) frequency as function of time during enzymatic treatment with 4.5 μM CBH I, CBH I Core and EG I (Figures S3, S4 and S5, respectively), XPS data of bi-component films enzymatically treated (Table S3);a XPS correlation plot for the % C-C surface concentration versus the O/C atomic ratio of the surface before and after enzymatic hydrolysis (Figure S6); and AFM 0.5 x 0.5 μm^2 height images of lignin films after enzymatic treatment with CBH I or EG I (Figure S7).

Purity of the enzymes

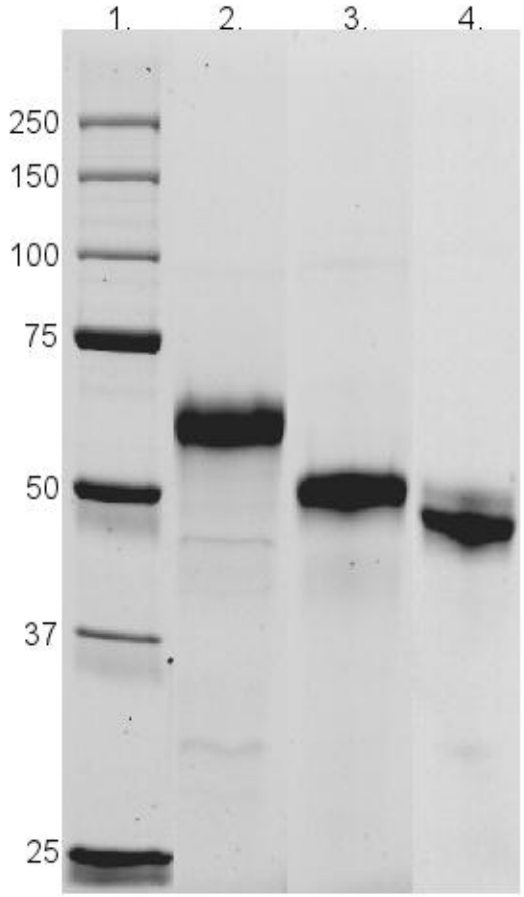

Figure S1. SDS-PAGE analysis of monocomponent cellulases: Lane 1. Mw standard; Lane 2. Cellobiohydrolase I; Lane 3. Endoglucanase I; Lane 4. Cellobiohydrolase I core. The size of each Mw standard band is shown in kiloDaltons (kDa). The image is constructed from several gel images.

Films characterization upon deacetylation

The morphology of the films before and after deacetylation was studied by AFM (Figure S2). CTA and AcL were initially solubilized in a common solvent (chloroform) as a single phase system; then, as the spin coating process proceeded and the solvent evaporated, the polymer concentration increased and the immiscible polymers underwent phase separation. Different evaporation rates are anticipated from the differences in the molecular weight and relative solubility between the respective

polymer and the solvent. Therefore, solvent-concentration gradient throughout the film were expected. The final morphology of the film depends on the initial total polymer concentration, blend ratio, spinning speed and polymer-polymer interactions, and could produce a bicontinous structure or isolated domains.[1, 2] According to previous work about phase separation phenomena in polymer blends,[3-5] AFM images of the films before deacetylation show a clear evidence of lateral phase separation of the bi-component polymer system that occurred during spin coating, due to the differences in miscibility upon solvent evaporation. As it was observed in the case of bi-component films from TMSC and AcL,[6] an increased AcL concentration in the blend promotes the formation of larger domains (CTA/AcL 1:1). After deacetylation, the roughness (measured by AFM and indicated in Figure 1 as Rq) of cellulose-containing films increased upon conversion of CTA to cellulose. This is likely due to the contraction of the CTA phase to a deswelled cellulose structure, which increases the differences in height between the various domains. However, the lignin films hardly showed changes in roughness upon deacetylation. The roughness of the Ce/L films decreased when the lignin content increased. A higher water contact angle (WCA, Figure S2) was observed with the increase in lignin content of the films, as expected.

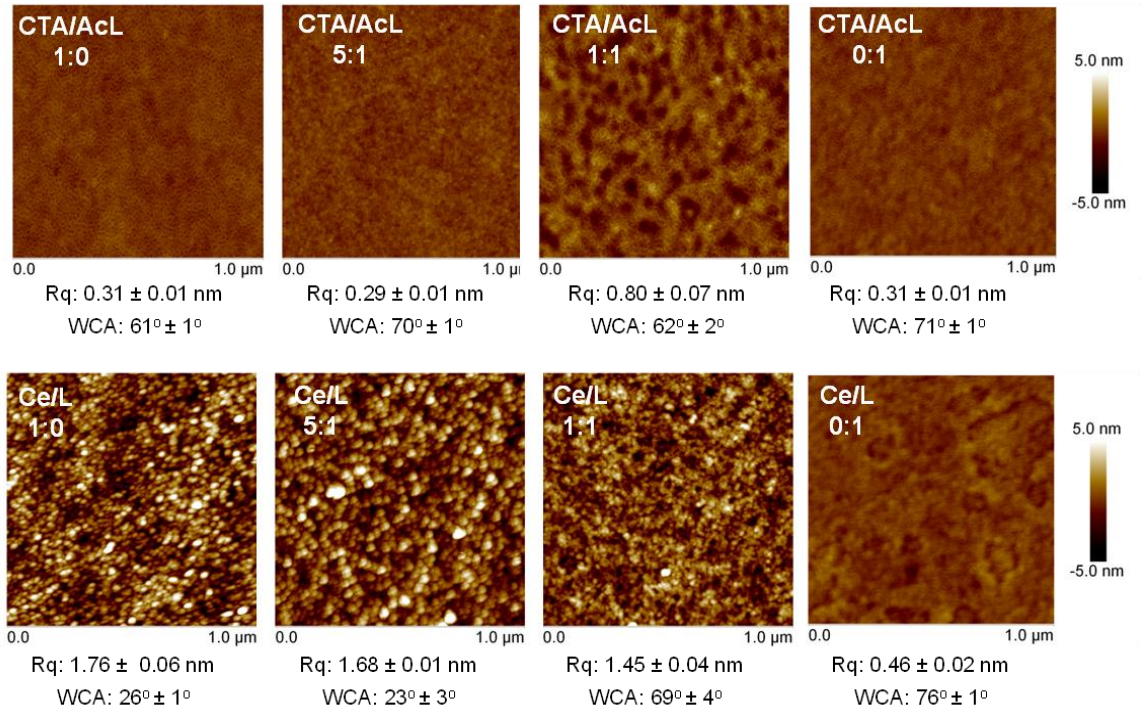

Figure S2. AFM 1x1 µm^2 height images of bi-component films before (CTA/AcL) and after deacetylation (Ce/L). The height scale (bar at the right of each image row) corresponds to Z values between -5 and +5 nm. Roughness (Rq) and water contact angle (WCA) of each film are also indicated.

Table S1. XPS data for bi-component films before (CTA/AcL) and after 68 hours of deacetylation treatment (Ce/L).

Film		Atomic Concentrations (%)				C 1s HiRes components (%)			
		O 1s	C 1s	N 1s	Si 2p	C-C	C-O	C=O	COO
CTA/AcL	1:0	36.3	63.7	0.0	0.0	27	39	10	24
	5:1	34.7	65.3	0.0	0.0	33	37	9	22
	1:1	29.9	70.1	0.0	0.0	45	34	6	16
	0:1	21.1	78.9	0.0	0.0	56	33	4	8
Ce/L	1:0	40.8	58.9	0.0	0.0	9	73	17	1
	5:1	35.9	63.4	0.7	0.0	21	64	15	1
	1:1	25.1	73.0	1.9	0.0	50	41	7	2
	0:1	18.7	78.6	2.7	0.0	59	30	3	2

Empirical models to quantify binding and hydrolysis. Independent empirical models for the extent and dynamics of binding and hydrolysis were used. In order to fit key kinetic parameters to the experimental results binding and hydrolysis data were fitted to an exponential decay equation and a Boltzmann-sigmoidal equation, respectively, according to Turon et al.[7]

The extent of binding and hydrolysis are described by the time-dependent (*t*, min) shift of the third overtone QCM frequency *Δf* (Hz), which was adjusted to equation s1 and s2, respectively. The binding parameters shown in equation s1 includes 1/ τ, the adsorption rate (min^{-1}) and, Mmax, the maximum binding value (Hz) corresponding to the minimum frequency measured. The hydrolytic parameters in Eq. s2 comprise the frequency at which hydrolysis ceases (*B*, corresponding to the plateau region at maximum frequency); the time for conversion to product to be maximized (V_{50}) and the hydrolysis rate (1/C).

$$\Delta f = M_{max}(1 - e^{-t/\tau}) \qquad (s1)$$

$$\Delta f = A + \frac{B-A}{1+e^{(V_{50}-t)/C}} \qquad (s2)$$

The adjusted parameters after enzyme treatment with 9μM solutions of CBH I, CBH I core and EG I are included in Table S2 (binding) and S3 (hydrolysis). When EG I was used, different behavior was observed, compared to CBH I or multicomponent enzymes solutions. Thus, the QCM profiles were divided in three segments in order to estimate the parameters that best describe each different stage of the process. Films in which lignin was the main component (1:1 and 0:1) presented a two phase adsorption process, so different parameters for each phase were calculated (EGI –F and EG – S in table S2 correspond to the fast adsorption observed in first place, and the slow adsorption, respectively). Films in which cellulose is the predominant component (1:0 and 5:1) presented a first small stage of hydrolysis before enzyme adsorption stage, so, the hydrolysis parameters corresponding to this stage were also estimated, and are indicated in Table S3 as EG I - FH.

Table S2. Model parameters describing the enzymatic adsorption on bi-component films upon treatment with CBH I, CBH I core and EG I 9μM solutions.

Ce/L Film + Enzyme	- M_{max} (Hz)	1/τ (min^{-1})	R^2
1:0 + CBH I	35.7	1.35	0.99
5:1 + CBH I	31.9	1.37	0.99
1:1 + CBH I	25.1	0.66	0.98
0:1 + CBH I	21.5	0.81	0.95
1:0 + CBH I Core	22.8	0.80	0.99
5:1 + CBH I Core	22.8	0.83	0.99
1:1 + CBH I Core	10.4	0.34	0.99
0:1 + CBH I Core	9.6	0.30	0.98
1:0 + EG I	10.9	0.10	0.97
5:1 + EG I	41.3	0.03	0.99
1:1 + EG I - F	14.7	1.46	0.98
0:1 + EG I - F	16.6	1.96	0.99
1:1 + EG I - S	34.5	0.03	0.99
0:1 + EG I - S	53.8	0.04	0.99

Table S3. Model parameters describing the enzymatic hydrolysis of bi-component films upon treatment with CBH I, CBH I core and EG I 9μM solutions.

Substrate	*B* (Hz)	V_{50} (min)	1/C (min^{-1})	R^2
1:0 + CBH I	85.0	47.6	0.032	0.97
5:1 + CBH I	51.2	34.6	0.039	0.96
1:1 + CBH I	20.1	47.9	0.042	0.98
0:1 + CBH I	6.6	38.2	0.047	0.99

1:0 + CBH I Core	34.9	56.9	0.036	0.98
5:1 + CBH I Core	26.3	58.0	0.036	0.98
1:1 + CBH I Core	4.8	65.1	0.030	0.99
0:1 + CBH I Core	0.7	52.8	0.053	0.92
1:0 + EG I - FH	10.1	0.41	5.25	0.99
5:1 + EG I - FH	1.2	0.58	3.79	0.94
1:0 + EG I	28.1	21.1	0.038	0.91
5:1 + EG I	12.2	55.2	0.026	0.97
1:1 + EG I	8.9	40.6	0.037	0.97
0:1 + EG I	2.6	17.0	0.187	0.86

QCM profiles upon enzymatic injection from 4.5 µM solutions (next page)

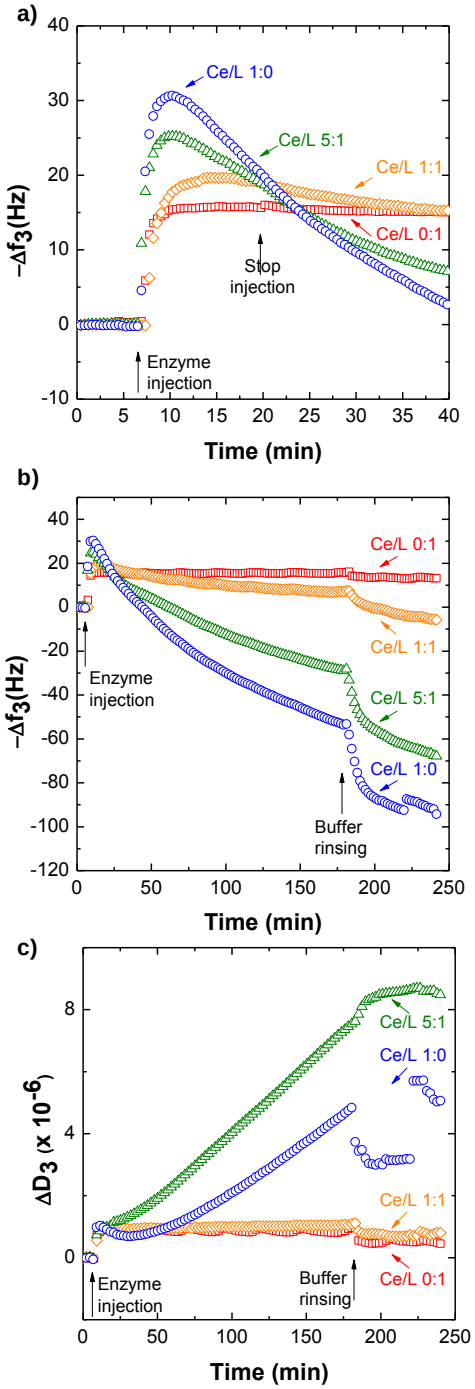

Figure S3. Negative shift in QCM frequency and changes in dissipation as a function of time after 15 minutes of continuous injection of a cellobiohydrolase CBH I (4,5 µM, flow rate of 100 µl/min) following by buffer (pH 5) rinsing as indicated by the vertical arrows. Profiles in (a) and (b) show the change in frequency for the first 40 minutes and the full time range (240 min), respectively. Data in panel (c) indicate the dissipation shift in the full time range.

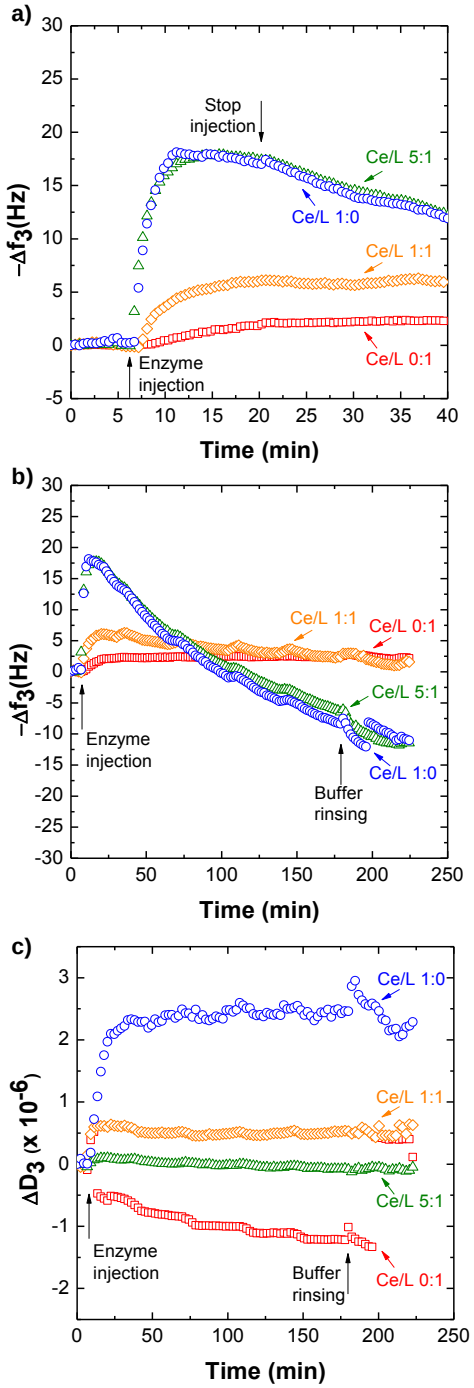

Figure S4. Negative shift in QCM frequency and changes in dissipation as a function of time after 15 minutes of continuous injection of a cellobiohydrolase CBH I core (4,5 µM, flow rate of 100 µl/min) following by buffer (pH 5) rinsing as indicated by the vertical arrows. Profiles in (a) and (b) show the change in frequency for the first 40 minutes and the full time range (240 min) respectively. Data in panel (c) indicate the dissipation shift in the full time range.

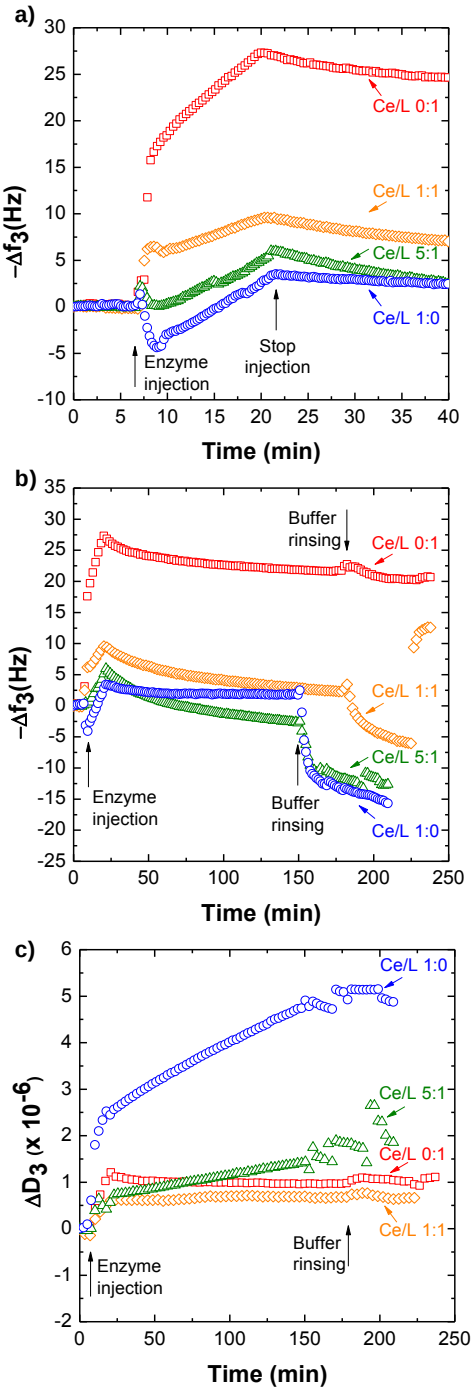

Figure S5. Negative shift in QCM frequency and changes in dissipation as a function of time after 15 minutes of continuous injection of a endoglucanase EG I (4,5 µM, flow rate of 100 µl/min) following by buffer (pH 5) rinsing as indicated by the vertical arrows. Profiles in (a) and (b) show the change in frequency for the first 40 minutes and the full time range (240) respectively. Data in panel (c) indicate the dissipation shift in the full time range.

XPS analysis of bicomponent films after enzymatic treatment

Table S3. XPS atomic concentration (O, C, N and Si) for lignocellullose films after enzymatic treatment with CBH I, CBH I core and EG I. Data corresponding to high resolution (HiRes) C atomic concentration are also included.

Film		Atomic Concentrations (%)				C 1s HiRes components (%)			
		O 1s	C 1s	N 1s	Si 2p	C-C	C-O	C=O	COO
CBH I	**1:0**	45.7	44.0	1.8	8.5	15	65	18	2
	5:1	34.6	56.0	3.7	5.7	41	43	13	3
	1:1	21.1	74.2	4.1	0.6	58	31	9	3
	0:1	18.9	75.7	5.1	0.4	61	29	7	3
CBH I core	**1:0**	37.9	59.7	2.3	0.0	14	67	17	2
	5:1	35.8	61.3	2.8	0.0	20	62	16	2
	1:1	20.0	76.3	3.7	0.0	62	30	5	3
	0:1	25.1	70.9	3.9	0.0	47	42	8	3
EG I	**1:0**	34.5	61.6	3.6	0.4	22	58	18	2
	5:1	30.9	66.0	3.1	0.0	32	51	15	2
	1:1	23.0	72.8	4.2	0.0	52	34	10	3
	0:1	17.4	77.0	5.6	0.0	62	27	9	2

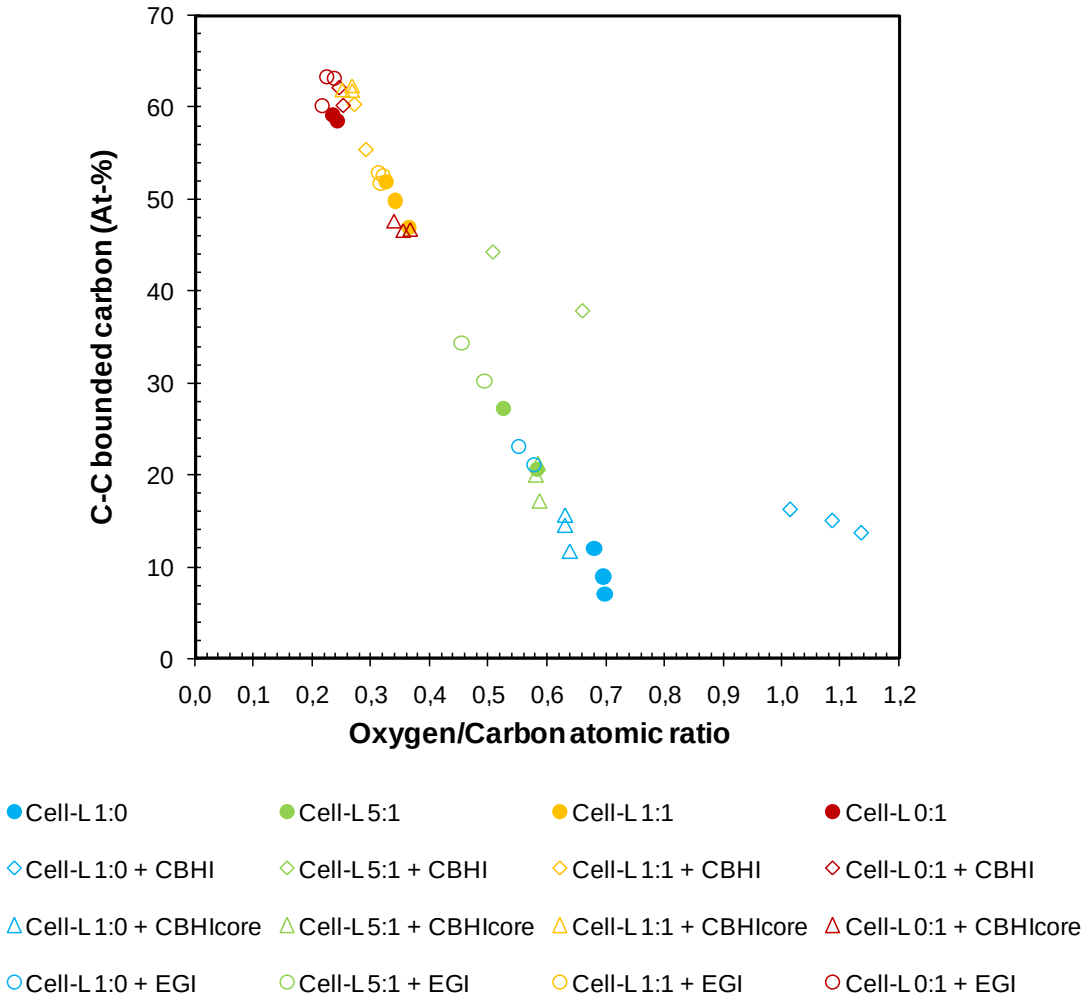

Figure S6. XPS correlation plot including the % C-C surface concentration *versus* the O/C atomic ratio calculated from XPS data in Table 2. Results for bicomponet films before (filled circles) are included along with those corresponding to the substrate after treatments with CBH I (empty diamonds), CBH I core (open triangles) or EG I (open circles).

AFM images of lignin films after enzymatic treatment

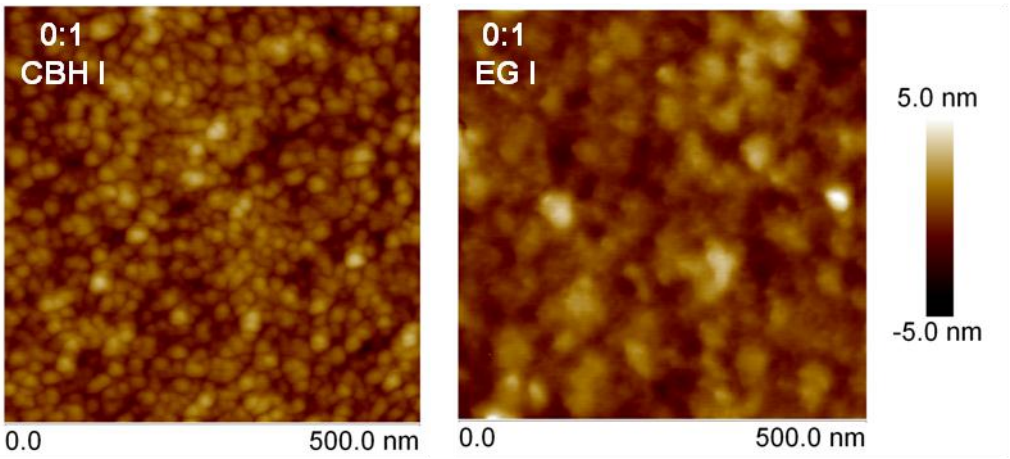

Figure S7. AFM 0.5 x 0.5 µm^2 height images of lignin films after enzymatic treatment with CBH I or EG I. The height scale (bar at the right of each image) corresponds to Z values between -2 and +3 nm. The respective line scan shown produced the height profile as indicated in the bottom panels.

REFERENCES

1. Inoue, T.; Ougizawa, T.; Yasuda, O.; Miyasaka, K. *Macromolecules* 1985, 18, 57-63.

2. Utracki, L. A., *Polym. blends handb.* Springer: 2003; Vol. 2.

3. Taajamaa, L.; Rojas, O. J.; Laine, J.; Kontturi, E. *Soft Matter* 2011, 7, 10386-10394.

4. Taajamaa, L.; Kontturi, E.; Laine, J.; Rojas, O. J. *J. Mater. Chem.* 2012.

5. Taajamaa, L.; Rojas, O. J.; Laine, J.; Yliniemi, K.; Kontturi, E. *Chem. Commun.* 2013, 49, 1318-1320.

6. Hoeger, I. C.; Filpponen, I.; Martin-Sampedro, R.; Johansson, L. S.; Österberg, M.; Laine, J.; Kelley, S.; Rojas, O. J. *Biomacromolecules* 2012, 13, 3228-3240.

7. Turon, X.; Rojas, O. J.; Deinhammer, R. S. *Langmuir* 2008, 24, 3880-3887.